Sound Particle Diffraction: Influence of angle and slit width discretisation as well as choice of diffraction coordinate system

Bestimmung des Einflusses der Parameter-Unsicherheiten innerhalb des Schallteilchen-Beugungs-Verfahrens

Stefan Weigand[1], Alexander Pohl[1], Uwe Stephenson[1]

[1] *HafenCity Universität, 20457 Hamburg, Deutschland, Email: stefan.weigand@hcu-hamburg.de*

Introduction

Diffraction is an important aspect of sound propagation, especially in urban areas or large halls, as receiver points are often only reached by this effect. Diffraction can be calculated analytically only for first order (e.g. the 'detour law' around screens) and numerically only for small scales or low frequencies (FEM, BEM) or, as combined with the inefficient mirror image source method, only for low orders [5].

The Sound Particle Diffraction (SPD) method based on the Uncertainty Relation (UR) has been in place for several years, too. Technically, to detect diffraction events, polyhedral rooms are divided into convex sub-rooms by polygonal apertures, so called virtual walls, at whose edges (inner edges of the room) diffraction takes place, i.e. on passing such a virtual wall, incident sound particles are split up into a set of S secondary sound particles (sSP). whose directions are evenly distributed on the half sphere beyond the virtual wall. The energy distribution of diffracted sSPs is governed by a Diffraction Angle Probability Density Function (DAPDF)[2] strongly depending on the estimation of the bypass distances to edges

In 3D, diffraction is calculated in two orthogonal planes. In each plane bypass distances and angles are estimated independently.

As calculating the sound particles' diffraction energies includes expensive numerical integration of the DAPDF, energies for some discrete sets of bypass distances and angle values are pre-calculated. First, the effect of this discretisation is quantified here. Second, the influence of the physically arbitrary choice of diffraction planes is discussed. Therefore different options are evaluated at four convex polygonal aperture shapes.

Sound Particle Diffraction based on the Uncertainty Relation

The basic principles are briefly repeated here: The model is: When a sound particle passes past an edge with bypass distance a, it *sees* a (thought) slit of width b. The slit width is proportional to a, yielding stronger deflection for closer bypass distances (see Abb. 1). The DAPDF is derived from octave band averaged Fraunhofer diffraction at a slit and is interpreted as an energy function for the sSPs[3]. It depends on the parameters slit width b (measured in the virtual wall, in wavelengths) and diffraction angle ε. A sSP with diffraction angle ε actually represents a sector $\Delta\varepsilon$. Thus its energy E is the integral of the DAPDF over sector $d\varepsilon$:

$$E(\Delta\varepsilon) = \int DAPDF(\varepsilon, b)d\varepsilon = \int \frac{D_0}{1 + 2 \cdot (2 \cdot b \cdot \varepsilon)} d\varepsilon \tag{1}$$

with normalizing constant D_0.

A function called Edge Diffraction Strength (EDS) is used to calculate the slit width of the (thought) slit from bypass distance a and coincident angle ε_1.

$$\frac{1}{b} := EDS(a, \varepsilon_1) = \frac{1}{6 \cdot a \cdot \cos(\varepsilon_1)} \tag{2}$$

If a sound particle passes several edges simultaneously (a slit) the individual EDS for each edge add up to a total-EDS: $TEDS = EDS_1 + EDS_2$.

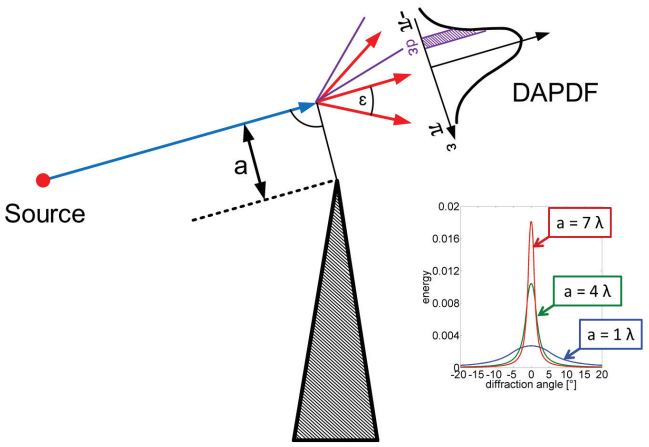

Abbildung 1: Basic principle of the Uncertainty Relation based Diffraction model.

The sound particles' energies are added up at some detector volumes around receiver points, as usual for the SPSM[1].

Extension to 3D

In 3D diffraction occurs in two independent orthogonal directions. E.g. a rectangular aperture can be interpreted as two orthogonal slits. Accordingly the uncertainty can be expressed in two orthogonal components A and B, too.

Thus the 3D-DAPDF is the product of two orthogonal 2D-DAPDFs in orthogonal directions A and B. Now the DAPDF is a function of four parameters: slit width b_A and diffraction angle ε in the A-plane and analogously b_B and η in the B-plane. The energy for a sSP with diffraction angles ε, η, representing the solid angle $d\Omega$ reads:

$$E(\Delta\Omega) = \iint DAPDF(\varepsilon, \eta, b_A, b_B)\, d\Omega \qquad (3)$$

Each slit width now depends on two bypass distances whose EDSs are added up as described earlier. As this integral has no analytical solution it needs to be solved numerically [3]. This is an expensive task. To avoid excessive computation time, energy values are pre-calculated for certain parameter sets and stored in a so-called diffraction database. Energy values for sound particles passing a virtual wall are then interpolated between these stored database values at runtime. *To evaluate the error due to this discretisation is scope of study I.*

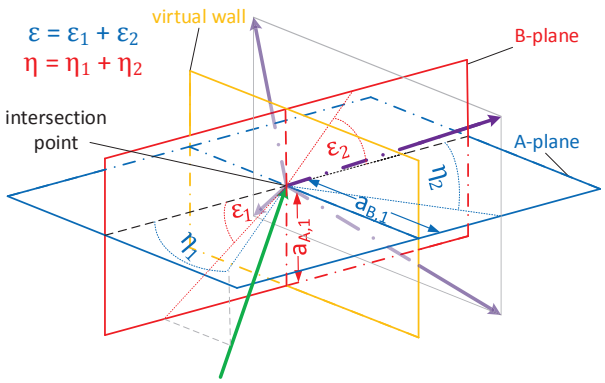

Abbildung 2: Example of 3D diffraction at a rectangular aperture: A sound particle (green) hits the virtual wall (yellow) and is split up into four secondary sound particles (sSP, purple). Two perpendicular diffraction planes A and B in which distances and angles are measured are shown in red and blue.

Choice of Diffraction Planes' Orientation

If non rectangular apertures are used, the choice of diffraction planes' A and B orientation becomes arbitrary. Several options are possible, two of which are sensible and thus described briefly using the example of a polygon with 7 edges (see Abb. 3)[3].

First option is to choose a fixed orientation, which is the same for all intersection points on one virtual wall (Abb.3, right). The orientation of the A-plane is parallel to an (arbitrary chosen) aperture's edge. This is a simple approach, however its results are not the closest distances to the edge, as assumed physically. Moreover a preferred direction is introduced.

Second option is to use an adaptive orientation, the planes' orientation is calculated for each intersection point independently (Abb. 3, left). The A-plane is in the direction of the shortest distance to the closest aperture's edge. This is closer to the physical meaning of uncertainty but leads to discontinuities at bisecting lines, as depicted in the figure (brown and dark blue plane orientations). For both options the B-plane is always perpendicular to the A-plane. *In study II these two options are evaluated at four aperture shapes comparing their performance to a wave theoretical solution (mentioned below).*

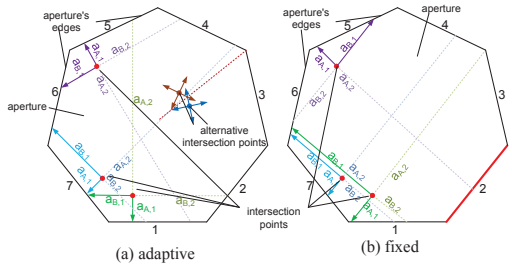

Abbildung 3: Examined options to orient diffraction planes. Adaptive orientation: diffraction planes are oriented for each intersection point individually, using the shortest distance to the closest aperture's edge. Fixed orientation: One orientation for all intersection points. The orientation is chosen parallel to one aperture's edge.

Numerical Studies

Two numerical studies were conducted. Study I was to examine the error due to interpolating secondary sound particles' (sSP) energy values from pre-calculated database values compared to continuous calculation at runtime. Study II evaluates the influence of the two discussed options for the diffraction planes' orientation on the diffraction result. Both options are applied to four convex polygonal aperture shapes (see Abb.5). Their results are compared to a wave theoretical reference given by Svensson's Edge Diffraction Tool Box (EDB)[4], based on his Secondary Source Model (SSM)[5].

Results of all studies are transmittance levels $L_i = 10\lg\left(\frac{I_{test}}{I_{freefield}}\right)$ and for comparison transmittance level differences $\Delta L_i = L_{test} - L_{ref}$ at 100 receiver positions (see Abb. 4).

Set-Up

The virtual wall is in the $y-z$-plane at $x = 0\,\mathrm{m}$. Spherical receivers with radius $r_r = 2\,\mathrm{m}$ are positioned on a 10×10 grid in a plane parallel to the virtual wall at $x = 10\,\mathrm{m}$ (beyond the virtual wall), spanning from $-20\,\mathrm{m} < y, z < 20\,\mathrm{m}$. The omnidirectional source is positioned at $So_1(-10\,\mathrm{m}, 0\,\mathrm{m}, 0\,\mathrm{m})$, unless noted otherwise. All surfaces are full absorbent.

Numerical simulations were conducted with 50000 primary sound particles and 2000 sSP. Simulations are done in third octave bands from 20 Hz to 20 kHz at once.

I: Effect of discretised DAPDF values

To examine and quantify the error due to discretisation, ten databases with different parameter discretisation

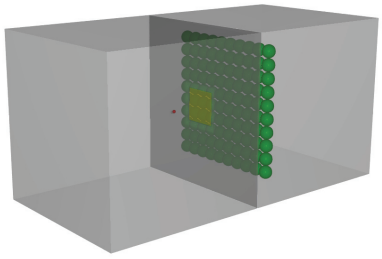

Abbildung 4: 3D view of the experimental set-up: Source (red dot) is 10 m in front of the virtual wall (yellow), representing the aperture. 100 spherical receivers with 2 m radius (green) are positioned on a 10×10 grid 10 m behind the virtual wall. All surfaces are full absorbing, yielding free-field conditions.

sets were defined. The results of these ten databases are compared to a reference which is simulated with continuously calculated sSP energy values under otherwise identical conditions. One discretisation set turned out to be the best compromise between accuracy and storage need. It was calculated with an angle resolution of 5° and logarithmically equidistant 25 slit width values between $b_{min} = 10^{-1}\lambda$ and $b_{max} = 10^{3}\lambda$. In the following, results for this last version are discussed only.

Simulations were done for two aperture shapes and two source positions yielding four scenarios. Examined aperture shapes are square and circular with side length and diameter $l = 10\,\mathrm{m}$, respectively. The circular aperture is approximated with a regular polygon ($n = 20$). In addition to So_1 the source is positioned at $So_2(-10\,\mathrm{m}, 5\,\mathrm{m}, -5\,\mathrm{m})$, too. Thus the four scenarios are a) square center; b) square corner; c) circular center; d) circular corner.

II: Effect of diffraction planes' orientation

To evaluate the influence of the two orientations discussed earlier, the Secondary Source Model [5] is used as reference. The SSM is based on edge sources, whereas here apertures are considered. So in setting the parameters of the SSM, as implemented in Svensson's Edge Diffraction Toolbox [4], outer edges need to be set far enough away (ca. 1000 λ) in order to not affect the results. While within the SPSM reflection and diffraction are handled strictly separately (ignoring boundary conditions), the SSM assumes hard flanking surfaces as boundary conditions. For reflections not to interact, the inner angles of the wedges are assumed to be practically 0 (1°).

For both options of diffraction plane orientation, four aperture shapes are realised (see Abb. 5). As simulations are carried out with several frequencies simultaneously, transmittance levels for 100 Hz, 1 kHz and 10 kHz are evaluated, yielding dimensions corresponding to ca. 3λ, $30\,\lambda$ and $300\,\lambda$, covering a reasonable range of wavelengths.

Results

Results of these studies are transmittance levels and transmittance level difference plots. To evaluate the results a metric is needed, preferably a single value metric. This is achieved by averaging the magnitude of ΔL over all receiver positions: $\overline{|\Delta L|} = \frac{1}{100}\sum_{i=1}^{100}|\Delta L_i|$.

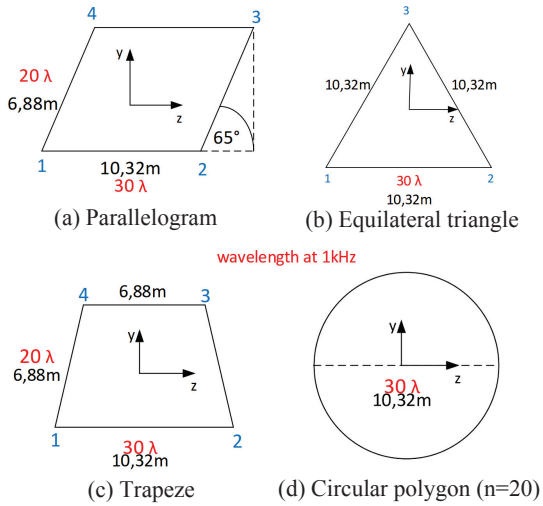

Abbildung 5: Shapes and dimensions of apertures examined in study II.

I: Effect of discretised DAPDF values

As a general measure for the error of discretisation Abb. 6 shows the arithmetic average over the absolute values of the differences between the discretised and the continuous results over all receiver positions as a function of frequency for all four scenarios a), b), c), d). Error rises with frequency, but stays below 0.7 dB. The errors of individual receivers are below 1 dB, even for 10 kHz (not shown). Scenario a) performed better than the other three scenarios, yet there is no principle dependency on shape or source position.

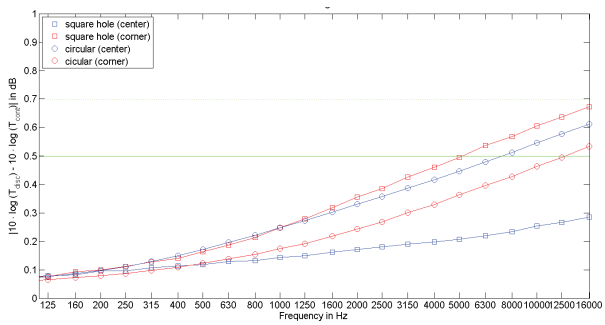

Abbildung 6: Results of study 1 examining the effect of discretisation using a database with pre-calculated DAPDF values and interpolation instead of continuous calculation at runtime for a square and circular aperture.

II: Effect of diffraction planes' orientation

Abbildung 7 shows three transmittance level maps. First, in the map for fixed option, the expected introduction of a preferred direction is visible, distorting the symmetry. Moreover the preferred direction hinders diffraction in certain directions (dark blue corners). The adaptive option performs quite well. The general structure is pre-

served, although the light green (ca. −20 dB) region is slightly too large.

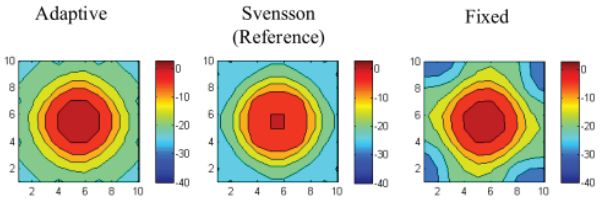

Abbildung 7: Colour-coded transmittance level (L) map from 0 dB to −40 dB for circular 20-polygon the adaptive option, Svensson-reference and fixed option (left to right) at 1 kHz.

In Abb. 8 three similar maps are shown for the triangular aperture, however the third one is a transmittance level difference (ΔL)-map in the range of −6 dB to 6 dB instead of the fixed option L-map. It is obvious, that the SPD has difficulties in the double shadow region (dark blue in the reference plot). The difference map indicates that the UBD generally tends to diffract too much (up to 2 dB) energy (yellow and orange regions) for all regions except the double shadow regions, where larger differences occur.

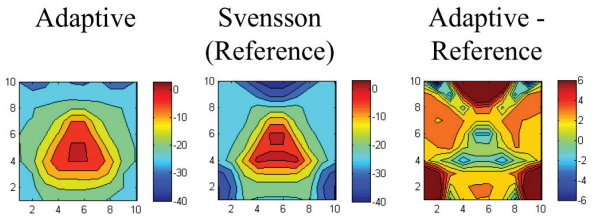

Abbildung 8: Colour-coded transmittance level (L) map from 0 dB to −40 dB and one colour map of ΔL from -6 dB to 6 dB for adaptive option, Svensson-reference and fixed option (left to right) at 1 kHz for the triangular aperture. Larger values are binned to maximum value.

The graph depicted in Abb. 9 shows the metric $\overline{|\Delta L|}$ defined before with circular marks for the adaptive (blue) and fixed (red) option. Moreover, bar plots indicate minimum and maximum values for ΔL. Data is organized in three blocks, each representing one frequency. The pictograms on the x-axis show the evaluated aperture's shape.

Although the minimum and maximum differences show large values, especially for high frequencies, one must keep in mind that these large deviations occur in regions where the transmittance level is on the order of −30 dB and less.

Conclusion

Study I showed that using a database with pre-calculated diffraction energies introduces only very small errors. The averaged errors is below 0.7 dB in the whole frequency range and is thus negligible. Maximum individual receiver errors are below 1 dB, too. Study II showed, that the adaptive orientation the diffraction plane performed better at all aperture shapes examined. Mean errors are in

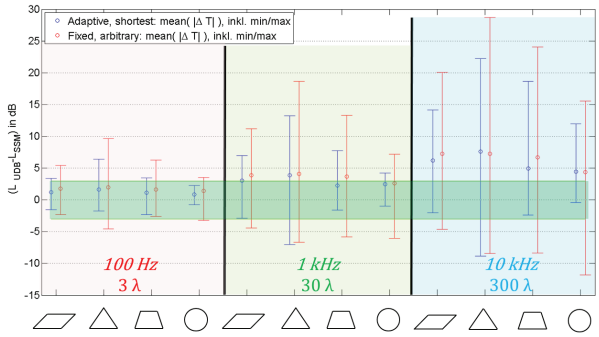

Abbildung 9: Results of study II examining performance of two examined options to orient diffraction planes. Displayed are differences in transmittance levels $\Delta L = L_{UDB} - L_{SSM}$ averaged over all receivers for the examined diffraction plane orientations (adaptive: blue, fixed: red) for three frequencies (100 Hz, 1 kHz, 10 kHz). Circular marks show $\overline{|\Delta L|}$, the error bars show minimum and maximum differences. Green bar indicates ±3 dB.

an acceptable range for low and medium frequencies relevant to diffraction. Some larger deviations can be found for large, hence seldom diffraction angles. Results are expected to improve with a new DAPDF developed recently.

Comparison with a wave theoretical model shows good agreement. Thus sound particle diffraction based on the uncertainty relation has taken another step to fully model sound propagation.

To simulate higher order diffraction in complex geometric scenarios, without explosion of computation time, the combination of the SPDM with the Sound Particle Radiosity Method (SPRAD) (re-unification of sound particles) is necessary[6].

Literatur

[1] Stephenson, U.: Comparison of the Mirror Image Source Method and the Sound Particle Simulation Method. Applied Acoustics (1990), 35-72

[2] Stephenson, U.: An Energetic Approach for the Simulation of Diffraction within Ray Tracing Based on the Uncertainty Relation. ACUSTICA (2010), 516-535

[3] Pohl, A.: Simulation of Diffraction Based on the Uncertainty Relation. PhD thesis, Hamburg, 2014

[4] Svensson Edge Diffraction Toolbox, URL: `http://www.iet.ntnu.no/~svensson/software/index.html`

[5] Svensson, P. et al: An analytic secondary source model of edge diffraction impulse responses. JASA (1999), 2331

[6] Pohl, A.; Stephenson, U.M. A combination of the sound particle simulation method and the radiosity method. Building Acoustics (New Zealand), 2011